RSC Advances

ROYAL SOCIETY OF CHEMISTRY

www.rsc.org/advances

Journal Name

RSCPublishing

ARTICLE

Mass Spectrometric Investigation on the Roles of Several Chemical Intermediates in Diamond Synthesis

Cite this: DOI: 10.1039/xoxxoooooox

Received ooth January 2012,
Accepted ooth January 2012

DOI: 10.1039/xoxxoooooox

www.rsc.org/

L. S. Fan,[a] Y. S. Zhou,[a] M. X. Wang,[a] Y. Gao,[a] W. Xiong,[a] Y. Liu,[a] Y. Lu,[a] J. F. Silvain[b] and Y. F. Lu[a],

Mass spectrometric studies were performed to investigate several key chemical intermediates and identify their roles in diamond synthesis in a $C_2H_4/C_2H_2/O_2$ combustion-flame chemical vapour deposition process. The diamond deposition rate and diamond quality were correlated with the growth parameters, the distance from the substrate to the torch nozzle and the oxygen-fuel ratio. The dependences of the intermediate concentrations as the functions of the distance to the torch nozzle and oxygen-fuel ratio were established. It was suggested that an appropriate balance between high hydrocarbon intermediates ($C_2H_2^+$, $C_3H_3^+$, $C_3H_4^+$, $C_4H_2^+$, $C_4H_3^+$) and carbon etchants (O^-, OH^-, and H_3O^+) was required to achieve effective diamond deposition. Influence of the resonant vibrational excitation of ethylene molecules in the diamond deposition was investigated. The resonant vibrational excitation stimulated the formation of high hydrocarbon intermediates while suppressed the yield of carbon etchants, which suggested the possibility in modifying the combustion process in a way that favoured the diamond synthesis through resonant vibrational excitation.

Introduction

Chemical vapour deposition (CVD) of diamonds has been extensively studied and successfully commercialized.[1-3] Due to its simplicity and high growth rate, combustion CVD using an oxy-acetylene flame has received considerable attention in growing diamonds since its discovery by Hirose *et al.*[4] Extensive investigations have been carried to understand the CVD diamond formation process and identify key chemical intermediates influencing the diamond growth process.[5-29] Three major plasma diagnostic techniques have been used to identify the active intermediates during diamond growth: laser-induced fluorescence (LIF),[5-8] optical emission spectroscopy (OES),[4,9-13] and mass spectrometry (MS).[5-8,14-17] L.C. Chen suggested C_2 as the key growth species in a hydrocarbon-rich environment based on the good agreement between C_2 and the diamond deposition rate observed in OES.[9] Y. Hirose suggested that OH plays an important role in the diamond growth via removing non-diamond carbon.[4] A.G. Lowe observed that the maximum of atomic H fluorescence intensity coincided with the good diamond growth conditions, confirming the positive role of atomic H in the diamond growth.[5] Although optical spectroscopy has a high resolution and sensitivity, some species, such as C_2, CH and OH, produce intensive emission due to electron-impact excitation even at a concentration far too low to account for the measured growth rates whereas most of hydrocarbon intermediates are not accessible using optical spectrometric methods due to lack of prominent visible emission bands.[5] Thus mass spectrometry has been used as a complementary method for a complete picture of the gas phase, especially in the aspect of identifying hydrocarbon intermediates.[5-8,14-17] Some generic features are shared by most diamond CVD systems, including: 1) presence of atomic H in superequilibrium; 2) dissociation of carbon-containing precursor gases; 3) moderate substrate temperature (800-1000 °C).[1-2] However, there has been a long-time debate on the roles of hydrocarbon species. Methyl radical, CH_3, is widely accepted as the growth species in hot-filament CVD (HFCVD) and microwave plasma CVD (MPCVD) systems.[14,19] Although numerous theoretical modelling confirmed that CH_3 plays a critical role in diamond growth,[22-25] there is still different voice.[26] M. Frenklach proposed a growth mechanism assuming

C_2H_2 is the key species,[26] which was also persistently observed in experiments.[7,16,19] The debates about which is the key growth species becomes even more intense in combustion CVD system due to the involvement of oxygen. Mass spectrometric studies of the oxyacetylene flames showed very weak or even no CH_3 signals, indicating CH_3 cannot solely account for the growth rate.[13,16] Several reports have indicated a significant role of high hydrocarbons in diamond growth.[5,21] Up to now, the mechanism of diamond formation has not yet been fully understood. Tailoring the gas phase chemistry in a way that favours the diamond growth requires in-depth understanding of the growth mechanism. Persistent efforts are thus required on the gas phase chemistry study in CVD of diamonds. As far as the combustion-flame CVD is concerned, a number of charged chemical intermediates are present in oxy-acetylene flames, which is proportional to the corresponding neutral radicals.[30] Identification of their roles in diamond growth process is crucial for the understanding of the diamond growth mechanism.

In this study, diamond growth using $C_2H_4/C_2H_2/O_2$ flames was studied as the functions of the flame positions and gas compositions. Mass spectrometric (MS) studies were conducted investigating the $C_2H_4/C_2H_2/O_2$ flames to explore the key chemical intermediates in diamond synthesis. Information retrieved through MS provided perspective insights into the gas phase chemistry of the combustion-flame CVD diamond deposition. A well-defined relation between several active intermediates and diamond growth was established based on the changes of hydrocarbons and carbon etchants with regard to the flame positions and gas compositions. A kinetic balance between the growth and etching of diamond and graphitic carbon was established during the diamond formation process. In previous studies, fast growth of diamond pillars with an average growth rate of 139 μm/h was achieved using the $C_2H_4/C_2H_2/O_2$ flames under resonant vibrational excitation of ethylene molecules,[31] and ascribed to a high-efficiency energy coupling due to the resonant vibrational excitation of the CH_2-wagging mode (a Type *c* fundamental band, υ_7, at 949.3 cm^{-1}) in ethylene molecules.[32] Influence of the laser excitations on the combustion flames was investigated using MS. The resonant vibrational excitation stimulated the formation of high hydrocarbon intermediates and suppressed the yield of carbon etchants, which revealed the important roles of the intermediates in diamond synthesis and suggested the possibility in modifying the combustion processes with the resonant vibrational excitation.

Experimental

The experimental detail for diamond deposition using $C_2H_4/C_2H_2/O_2$ combustion flames has been reported in previous study.[31] Surface morphologies of the diamond films were characterized by a scanning electron microscope (SEM; XL-30, Philips Electronics). Diamond qualities were evaluated using a micro-Raman spectrometer (inVia, Renishaw). An argon-ion laser with a wavelength of 514.5 nm and a power of 50 mW was used as the exciting source. Diamond film thickness was measured using a stylus surface profiling system (XP-2, AMBiOS) with a stepping speed of 0.05 mm/sec. The experimental setup for the MS studies is schematically shown in Fig. 1. Ionization of intermediates occurs in the combustion flames, making the flames suitable for direct analysis using MS. A.N. Hayhurst performed a comprehensive study of ions in oxyacetylene flames and suggested an ion concentration of 10^{11} ions/cm^3 in a pool of 10^{18} molecules/cm^3.[30] An ionization degree of 10^{-7} is therefore expected in our work. Charged ions reflect the presence of corresponding neutral species and proportional to their concentrations in the flame. Thus, charged ions in our work acted as proxies for the corresponding neutral species. Combustion flames were produced by a gas mixture of C_2H_4, C_2H_2, and O_2 with flow rates of 35, 35 and 60 - 80 standard cubic centimetres per minute, respectively. Both positive and negative ions in the flames were detected using a time-of-flight mass spectrometer (MS, AccuTOF^{TM}, JEOL USA, Inc.). A stainless steel orifice with an inner diameter of 400 μm was used to collect ions from the flames in open air. A wavelength–tunable CO_2 laser (PRC Inc, 9.2 ~ 10.9 μm) was used to irradiate the $C_2H_4/C_2H_2/O_2$ combustion flames. C_2H_4 was added to achieve efficient laser energy coupling by resonantly exciting the CH_2-wagging vibrational mode.[32] The laser beam was normally projected through the flame at the torch nozzle with a focused diameter of ~ 2 mm. The temperature distribution shows a drastic spatial gradient inside the inner cone of the combustion flame. The gas temperature at the torch nozzle is generally at around several hundred kelvins since the ignition just initiates at this point,[33-34] while the temperature at the middle of the inner flame could reach as high as 3000 K. To ensure sufficient thermal population at the ground state available for excitation, the laser beam was directed into the flame at the torch nozzle where the precursor gas temperature is much lower than the middle part of the inner flame, as indicated in Fig. 1. The laser incident power was 100 W. The combustion torch was fixed on a motorized 3D stage. The relative position of the flames to the orifice was precisely controlled at a resolution of 2.5 μm. The mass range investigated was from 10 to 60 m/z. The MS data were analysed using the TSSPro software (Shrader Analytical and Consulting Laboratories, Inc. Version 3.0) and the MS Tools software (JEOL USA, Inc.). An unperturbed $C_2H_4/C_2H_2/O_2$ flame structure is shown in Fig. 1. There are three distinct regions in a flame: (a) inner flame, (a) feather region, and (3) outer diffusion flame. Diamond was obtained within a narrow area in the feather region right below the inner flame tip, which is named as the "tip" region in the following discussion. As an important parameter, the distance from the sampling orifice to the torch nozzle is defined as *h* in the following discussion. A suitable *h*, from 3.1 to 3.5 mm, was required to achieve an effective diamond deposition.

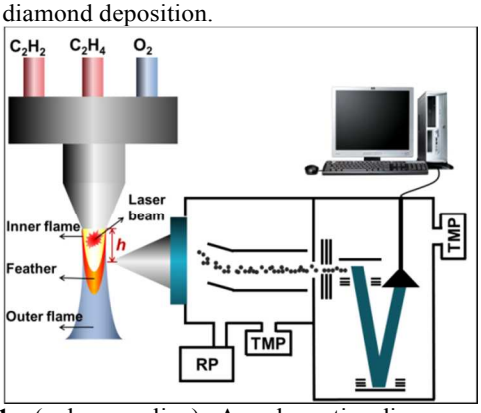

Figure 1. (colour online) A schematic diagram of mass spectrometric investigation of the $C_2H_4/C_2H_2/O_2$ combustion flames. RP represents rotary pump; and TMP represents turbomolecular pump.

Results and Discussion

Mass spectrometric measurement

In order to understand the diamond formation process, MS investigations on the combustion flames were performed. Figure 2 exhibits two typical mass spectra obtained for positive, Fig. 2(a), and negative, Fig. 2(b), ions in the $C_2H_4/C_2H_2/O_2$ flames without laser irradiation at the tip region (h = 3.3 mm), where diamond films were obtained. Each line was assigned to an ion in the flames. Ion identification adopted the chemical assignations suggested in Ref [15]. Due to the increased uncertainties at higher mass numbers, only ions in the range of 10 - 60 m/z were investigated. The relative concentration of each ion was derived by dividing its intensity with the total ion count value in order to eliminate the variation of its absolute value in different measurements.

In the mass spectrum of positive ions, large quantity of hydrocarbons ($C_xH_y^+$, x = 1 - 4, y = 1 - 4) were identified whereas H_3O^+ was the most abundant species. In the mass spectrum of negative ions, carbon etchants, O^- and OH^- were identified. Oxidization products, including H_3O^+, OH^-, and O^- were critical carbon etchants in diamond growth. H_3O^+ ions were produced by adding a proton to each H_2O molecule, reflecting the formation of neutral H_2O molecules during the combustion process. The thermochemical etching effect of H_2O vapour on CVD diamond films was proved by N. Uchida and co-workers.[35] Numerous reports have reported that O^- and OH^- paly a similar etching role as atomic H in combustion synthesis of diamonds by preferentially etching the sp^2-hybridized graphitic carbon and stabilizing the sp^3-hybridized carbon phase.[4,5,10,16]

The persistence of $C_xH_y^+$ ions indicated the presence of large quantity of hydrocarbon intermediates in the flames. Although hydrocarbons was suggested to be responsible for the diamond growth, there has been a long-time debate over the question which hydrocarbon species is the key growth species, Y. Matsui measured the gas concentration in oxyacetylene flame using MS, in which C_xH(x=1,2), C_x(x=1-3) and CH_x(x=1-3) were dominant C-radicals.[13] However he excluded most of them as growth candidates based on two criterions: superequilibrium and sufficient concentration.[13] C_2H_2 was also excluded due to the disagreement of R-dependency.[13] C.A. Wolden studied the flat flame using MS.[16] He suggested the role of C_2H_2 as growth species due to the decrease of C_2H_2 with the oxygen-fuel ratio,[16] which is apparently contrary to Y. Matsui's opinion.[13] A.G. Lowe performed species concentration measurement in oxyacetylene flame.[5] Although CH_3 was observed in the mass spectrum, its low concentration discounted the significance in diamond growth.[5] Meanwhile, higher hydrocarbons in substantial quantities was suggested an active role in diamond growth.[5] Similar suggestion was also made by S.J. Harris.[21] The relative concentration of CH_3 for good diamond growth conditions was below 0.25% in our study. As concluded from the previous studies, CH_3, which is commonly accepted as the growth species in diamond deposition, was found inadequate to account for the growth rate in combustion CVD of diamonds. A variety of hydrocarbon could act as a growth species for diamond deposition. The ion, O_2^-, was formed by attaching an electron to an oxygen molecule, which reflected the consumption of oxygen in the gas mixture and showed little impact on the diamond formation. Other ions, like CO^+, CO_2^+, NH_4^+, CN^- and C_2O^-, were also detected in MS with much lower concentrations. CO^+, CO_2^+, and C_2O^- are ultimate products of the combustion process and do not exhibit obvious influence in diamond deposition, while NH_4^+ and CN^- are by-products when reacting with nitrogen in the air.

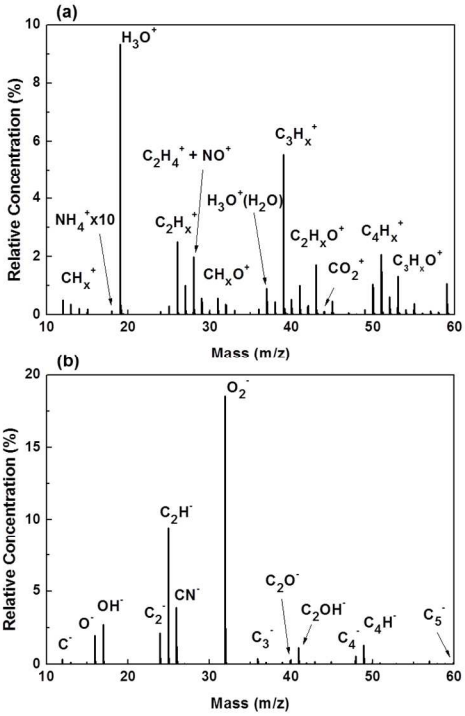

Figure 2. Typical mass spectra of positive (a) and negative (b) ions in the combustion flames at the tip region (h = 3.3 mm).

The diamond deposition was highly sensitive to the distance h and oxygen-fuel ratios. Diamond films were obtained only within a narrow tip region with a hydrocarbon-rich precursor mixture. Experimental parameters, h and the oxygen-fuel ratio, $R = O_2 / (C_2H_2+C_2H_4)$, were varied in diamond growth and MS characterizations. The MS results were analysed in the region: R = 0.85 - 1.10 and h = 2 - 5 mm.

Diamond growth and MS as the functions of h

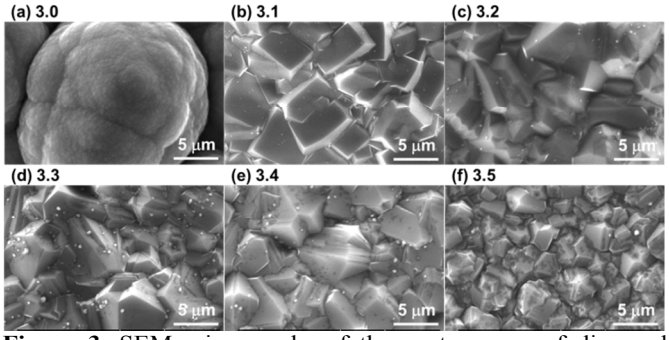

Figure 3. SEM micrographs of the centre areas of diamond films deposited with a distance h from the substrate to the torch nozzle of: (a) 3.0, (b) 3.1, (c) 3.2, (d) 3.3, (e) 3.4, and (f) 3.5 mm.

The distance h between substrates and the torch nozzle played a critical role in diamond deposition. When the substrate was moved from the inner flame through the feather region towards the outer diffusion flame, the carbon deposition channel

transited from amorphous carbon to diamond and then to no deposition. Figure 3 shows SEM micrographs of the centre areas of diamond films deposited at different h values. With a substrate placed right at the inner flame tip (h = 3.0 mm), films with amorphous ball-like structures in the centre area were obtained due to fast accumulation of non-diamond carbons (see Fig. 3(a)). As the substrate moved downwards to h = 3.1 mm, {100}-faceted diamond particles were observed (see Fig. 3(b)). As h further increased from 3.2 to 3.5 mm, diamond grains in random orientations were observed (see Fig. 3(c)-(f)). The grain size decreased with an increasing h value.

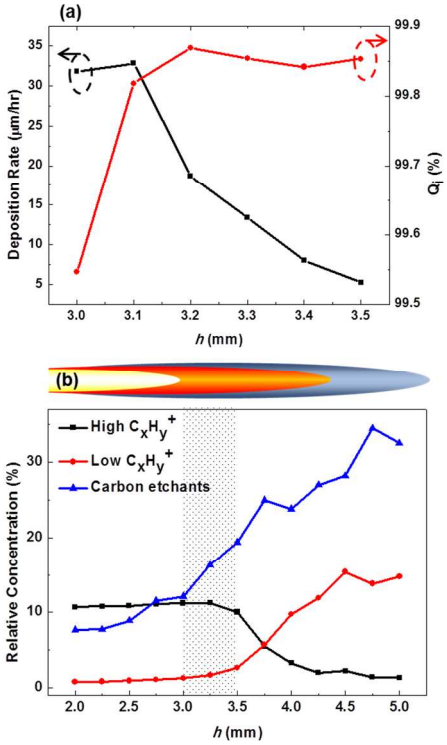

Figure 4. (colour online) (a) Deposition rates (black solid squares) and diamond qualities (red solid circles) plotted as a function of the distance h. (b) Overall relative concentrations of three types of intermediates plotted as a function of h. The dashed area is the diamond deposition region.

The deposition rate was calculated via dividing the film thickness by the deposition time. The diamond films were characterized using Raman spectra (Fig. S1). To analyse the diamond quality, a quality factor $Q_i = I_{diamond} / (I_{diamond} + I_{a\text{-}carbon} / 233)$ was derived from the Raman spectra, with $I_{diamond}$ and $I_{a\text{-}carbon}$ being the intensities of the diamond peak (1337 cm^{-1}) and the sum of the intensities of the non-diamond carbon peaks (D-band: 1370 cm^{-1} and G-band: 1550 cm^{-1}), respectively.[38-40] The deposition rates and diamond qualities are plotted as a function of h in Fig. 4(a), which show opposite variation trends. The deposition rate exponentially decreased as h increased from 3.2 mm to 3.5 mm. The diamond quality was drastically improved as the substrate moved from h = 3.0 to 3.1 mm and then kept relatively constant with h ranging from 3.2 to 3.5 mm.

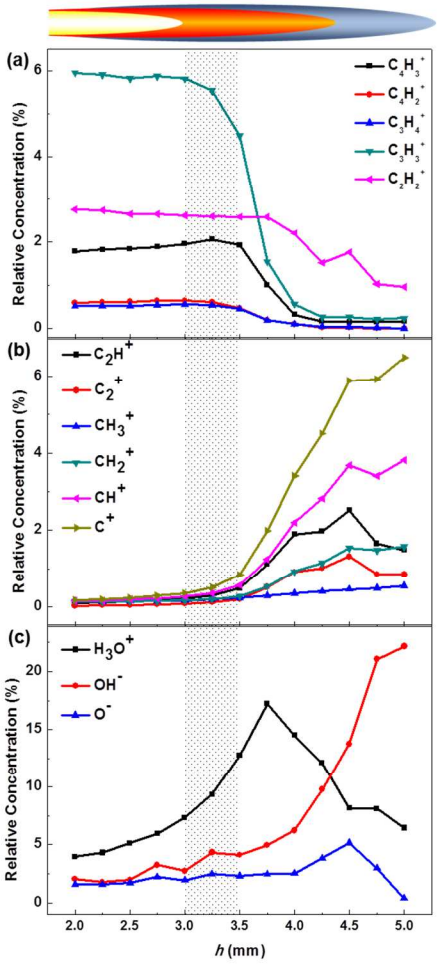

Figure 5. (colour online) Relative concentrations of (a) high hydrocarbons, (b) low hydrocarbons, and (c) oxidized products as a function of h. The dashed area is the diamond deposition region.

The chemical intermediates in the combustion flames at different h values were studied using MS. Investigations focused on two types of chemical intermediates: hydrocarbons and carbon etchants. The relative concentrations of chemical intermediates are plotted as a function of h at a gas ratio of R = 0.969 in Fig. 5. The gas ratio, R = 0.969, was the optimized value at which diamond films were obtained. Low hydrocarbons (C^+, CH^+, CH_2^+, CH_3^+, C_2^+, and C_2H^+) and high hydrocarbons ($C_2H_2^+$, $C_3H_3^+$, $C_3H_4^+$, $C_4H_2^+$, $C_4H_3^+$) exhibited different h-dependences. As shown in Fig. 5(a), high hydrocarbons were abundant in the inner flame. The relative concentration of high hydrocarbons began to decrease in the tip region, dropped quickly in the feather region, and fell below 2.0% in the out diffusion flame. With an opposite variation direction as shown in Fig. 5(b), the relative concentration of low hydrocarbons kept at a low level in the inner flame, began to increase in the tip region and increased quickly in the feather through the outer diffusion region. Among the low hydrocarbons, the relative concentration CH_3^+ was found below 0.25%, which cannot solely contribute to the observed deposition rates (~30 μm). The relative concentrations of carbon etchants (H_3O^+, OH^-, and O^-) increased from the inner flame zone to the feather zone. The relative concentration of H_3O^+ reached a maximum value in the middle of the feather

region. The reduction of the H_3O^+ concentration in the outer diffusion flame can be attributed to the electron-H_3O^+ recombination process: [41,42]

$$H_3O^+ + e^- \rightarrow \text{neurtral products.} \quad (1)$$

The relative concentration of O^- reached a maximum value at the end of the out diffusion region. A persistent reduction of OH^- was found from inner flame through the outer diffusion region. The relative concentrations of species in each category (high hydrocarbons, low hydrocarbons, and carbon etchants) exhibited similar variation trend. For a conclusion on the significance of them for the diamond growth, it is not sufficient to discussion their concentration alone. The relative concentrations of the species in each category were added up to obtain an overall variation trend for each category. This could present a comprehensive picture of the flame chemistry, providing direction for tailoring the CVD process to specific requirement. The overall relative concentrations of low hydrocarbons, high hydrocarbons, and carbon etchants were plotted as a function of *h* in Fig. 4(b).

The Russian school first proposed the idea that diamond growth is controlled by kinetic competition between graphite formation and diamond formation since sp^2-bonded carbon is more vulnerable to etchants than sp^3-bonded.[28] Both graphitic carbon (sp^2 hybridized carbon) and diamond carbon (sp^3 hybridized carbon) deposit simultaneously on substrate surfaces, and are etched concurrently by the carbon etchants. The deposition of diamond films is based on the fact that sp^3-hybridized diamond phase is more stable towards carbon etchants than sp^2-hybridized graphite phase.[29] The carbon etchants play double-bladed roles in the diamond deposition process. With a shortage of etchants, the growth speeds of graphite and diamond are faster than their etching rates, the net result is amorphous carbon deposition. When a moderate amount of etchants present in the gas phase, the etching speed of graphitic carbon is faster than its growth rate while the growth rate of diamond is higher than its etching rate, then the net result is diamond growth.[29] With excessive etchants, the diamond etching rate exceeds the diamond growth rate and the net result is deteriorated diamond deposition even no carbon deposition at all.[29] The variation of the carbon etchants (H_3O^+, OH^-, and O^-) with respect to *h* was therefore particularly interesting, as illustrated in Fig. 4(b). The overall relative concentration of carbon etchants (Fig. 4(b)) increased consistently as moving downstream from the inner flame to the outer diffusion flame. When the overall relative concentration of carbon etchants increased with an increasing *h* from 3.0 to 3.5 mm, the diamond quality (red solid circles in Fig. 4(a)) was drastically enhanced from h = 3.0 to 3.1, then remained relatively unchanged from h = 3.1 to 3.5, whereas a persistent decrease in diamond deposition rate (black solid squares in Fig. 4(a)) was observed. This result confirms the positive roles of carbon etchants in diamond synthesis by effectively removing graphitic carbon. It is also noted that further increase in the carbon etchant concentration could not improve the diamond quality apparently but led to a fast reduction of the deposition rate due to excessive etching of diamond.

Low hydrocarbons, including CH_3, CH, and C_2, in the gas-phase reaction were suggested to play active roles in diamond formation via providing carbons.[5,21] Both A.G. Lowe[5] and S. J. Harris[21] suggested a similarly active role for high hydrocarbons in the diamond deposition. Meanwhile, high hydrocarbons were suggested responsible for forming aromatic structures, which eventually leads to soot formation. The increase of low hydrocarbons, which showed similar variation trend with CH_3^+, coincided with the decrease of the deposition rate, suggesting a role like etchants rather than as growth species in diamond growth. The high concentration of low hydrocarbons, which was found in the outer diffusion region where no diamond grown, discounted the significance of low hydrocarbons in diamond growth. The decrease of the relative concentration of high hydrocarbons coincided with the decrease of the deposition rate, but also led to the improved diamond quality. High hydrocarbons which contribute for both diamond and non-diamond carbon growth played a double-bladed role. In the inner flame where there was a lack of etchants, the high concentration of high hydrocarbons led to co-deposition of both sp^2- and sp^3-hydridized carbon, amorphous carbon deposition occurred. The high concentration of high hydrocarbons with moderate amount of etchants in the tip region was responsible for the fast deposition of high quality diamonds. As the substrate moved downstream, the etchants became dominant while high hydrocarbons fell below 1%, the deposition rate reduced quickly due to the insufficient supply of carbon source. Based on our observations, high hydrocarbons with substantial quantity in the flames play a more significant role than low-hydrocarbons in the combustion CVD of diamonds.

Diamond growth and MS as the functions of gas compositions

Another important parameter in combustion diamond synthesis is the oxygen-fuel ratio, $R = O_2/(C_2H_2+C_2H_4)$. When R = 1.0, a neutral flame is achieved, which is also defined as the condition where the feather region just disappears because all the fuel gases are consumed in the inner flame. The flames with $R > 1$ are called oxygen-rich flames. When $R < 1$, hydrocarbon-rich flames are produced.[1] Hirose *et al.* published a map of diamond growth regimes versus to the O_2/C_2H_2 gas ratio, which suggests that diamond was obtained in a narrow O_2/C_2H_2 ratio range.[4] In this study, diamond films were deposited in the tip region in hydrocarbon-rich flames at an *R* value ranging from 0.922 to 1.

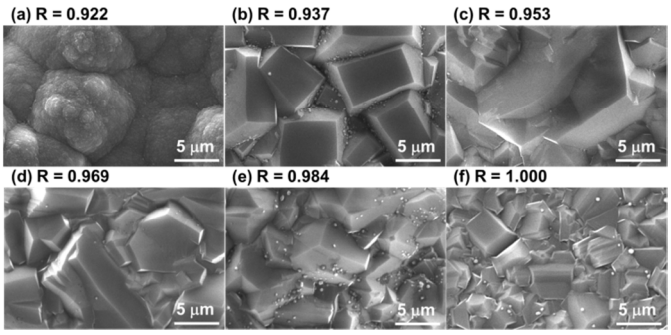

Figure 6. SEM micrographs of center areas of diamond films deposited with a gas composition (*R*) of: (a) 0.922, (b) 0.937, (c) 0.953, (d) 0.969, (e) 0.984, and (f) 1.

Figure 6 shows the SEM micrographs of diamond films deposited with *R* ranging from 0.922 to 1. At R = 0.922, amorphous ball-like structures were observed due to graphitic and amorphous carbon accumulation (see Fig. 6(a)). At R = 0.937, {100}-faceted diamond grains were deposited (see Fig. 6(b)). With *R* increasing from 0.953 to 1, the diamond grain orientation became random and the grain size decreased due to an insufficient carbon supply and excessive etching in oxidizing conditions (see Fig. 6(c)-(f)). The diamond films were characterized using Raman spectra (Fig. S2). The deposition

rates and diamond qualities are plotted as a function of *R* in Fig. 7(a). The diamond deposition rate reached a maximum value at *R* = 0.969 and reduced significantly with *R* increasing from 0.969 to 1. The diamond quality was obviously improved as *R* increased from 0.922 to 0.953 and kept relative constant with *R* higher than 0.953.

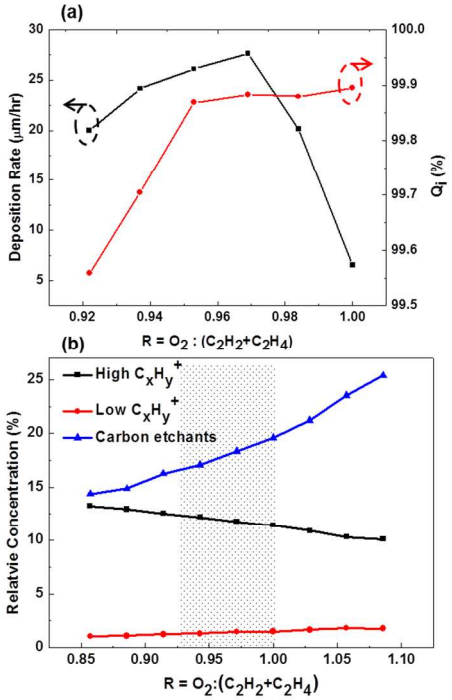

Figure 7. (color online) (a) Deposition rates and diamond qualities plotted as a function of *R*. (b) Overall relative concentrations of three types of intermediates plotted as a function of *R*. The dashed area is the diamond deposition region.

The relative concentrations of low hydrocarbons, high hydrocarbons, and carbon etchants are plotted as a function of *R* at *h* = 3.3 mm in Fig. 8. The relative concentrations of high hydrocarbons, including $C_2H_2^+$, $C_3H_3^+$, $C_3H_4^+$, $C_4H_2^+$, $C_4H_3^+$, reduced constantly from *R* = 0.92 to 1.0. Both low hydrocarbons (C^+, CH^+, CH_2^+, CH_3^+, C_2^+, and C_2H^+) and carbon etchants (H_3O^+, OH^-, and O^-) increased over this narrow range. The overall relative concentrations of the three types of intermediates are plotted as a function of *R* in Fig. 7(b). Over the *R* range, the overall relative concentration of low hydrocarbons increased but with a subtle increment. The decrease of high hydrocarbons and the increase of carbon etchants from hydrocarbon-rich flames (*R* < 1.0) towards oxygen-rich flames (*R* > 1.0) coincided with a growth transition from amorphous carbon to high quality diamond, then to etching of diamond. This result suggests that an appropriate ratio of carbon etchants and high hydrocarbons was required to realize diamond formation. A counterbalance between the growth and the etching of diamonds and graphitic carbon was required for growing diamond.

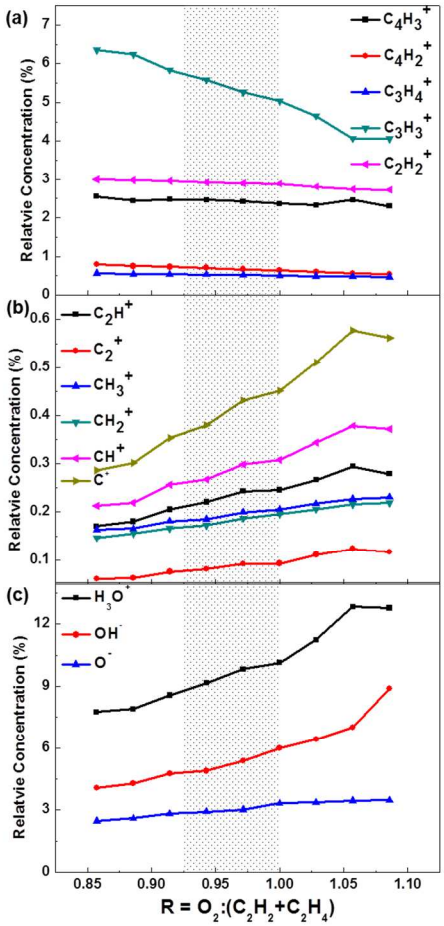

Figure 8. (colour online) Relative concentrations of (a) high hydrocarbons, (b) low hydrocarbons, and (c) oxidized products as a function of *R*. The dashed area is the diamond deposition region.

Diamond growth and MS with laser resonant excitations

It has been reported previously that resonant vibrational excitation of the v_7 umbrella band (CH_2-wagging mode) of ethylene molecules in the $C_2H_4/C_2H_2/O_2$ flames at a matching laser wavelength of 10.532 μm led to significantly increased diamond deposition rate and quality improvement.[44] Figure 9 shows the SEM images (Fig. 9(a) and (b)), film thickness profile (Fig. 9(c)) and Raman spectra (Fig. 9(d)) of diamond films obtained without and with resonant laser excitation. The diamond grain size, film thickness and diamond quality were significantly improved under resonant vibrational excitation compared with those without laser irradiations. As indicated in the insets of Fig. 9(a) and (b), the combustion flames shrank in length, expanded in diameter and became brighter under resonant vibrational excitations, which suggests that resonant vibrational excitations of ethylene molecules modified the combustion process in a way that coupled energy into the chemical gas phase, increased the flame temperature and accelerated the combustion reactions.

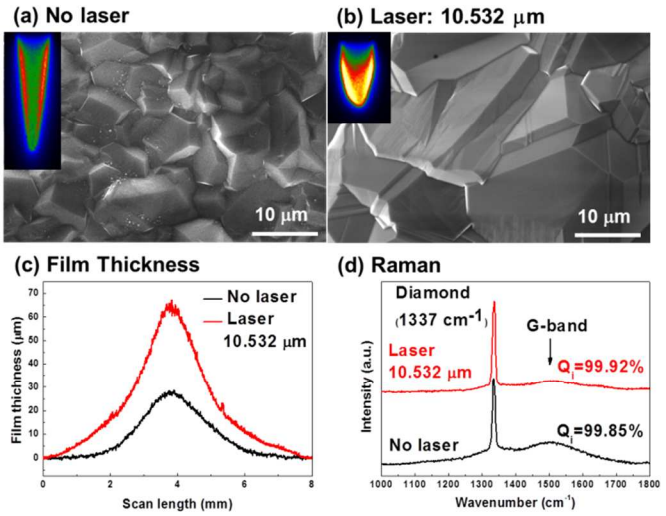

Figure 9. SEM micrographs of diamond films deposited (a) without and (b) with laser resonant excitation at a laser wavelength of 10.532 μm; insets are the optical images of the combustion flames without and with laser excitations, respectively. (c) Film thickness profiles and (d) Raman spectra of the diamond films.

In order to understand the effects of laser excitations on the combustion diamond deposition process, the $C_2H_4/C_2H_2/O_2$ combustion flames under laser irradiations at different laser wavelengths cantered at 10.532 μm were studied using MS. Figure 10 shows the overall relative concentration of the intermediates as a function of incident laser wavelengths at h = 3.3 mm and R = 0.969. The overall relative concentration of high hydrocarbons reached a maximum point (12.1%) whereas the overall relative concentration of carbon etchants was in minimum (14.7%) at 10.532 μm. No obvious variation was observed for low hydrocarbons. The species concentration variations with regard to the laser wavelength can be attributed to the modified combustion processes under laser excitations.[29] As evidenced in the previous study, the flame temperature under laser irradiation increased as laser wavelengths approached 10.532 μm.[44] As shifting away from the centre frequency of the v_7 fundamental band (10.534 μm), the excitation became off resonance. Resonant vibrational excitation was more effective than off-resonance excitations in energy coupling and modifying the combustion processes. As discussed above, high hydrocarbons exhibited a good agreement with the deposition rate upon the control parameters and a positive role in promoting diamond formation was suggested for high hydrocarbons therefore. The maximum high hydrocarbon concentration under the resonant vibrational excitation indicates that the flame chemistry was modulated to favour the fast diamond deposition. The low concentration of carbon etchants leads to a low diamond etching rate and a fast diamond deposition speed at 10.532 μm. The variation of the flame chemistry with laser excitations demonstrates that resonant vibrational excitations could modulate the chemical species distribution in a way that facilitated diamond synthesis. A proper modulation of the ratio of high hydrocarbons and carbon etchants within the diamond formation region could efficiently steer the reactive channel towards diamond formation and promote the diamond deposition rate.

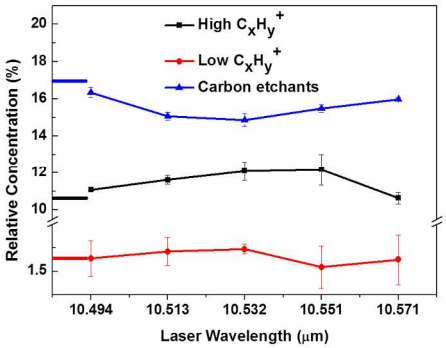

Figure 10. (colour online) Overall relative concentrations of three types of intermediates plotted as a function of incident laser wavelengths. The color-coded solid bars inside indicate the relative concentrations of the corresponding species without laser irradiation.

Kinetic growth mechanism

The diamond growth was suggested to be controlled by kinetic competition between graphite and diamond formation since sp^2-bonded carbon is more vulnerable to etchants than sp^3-bonded.[28] Although this kinetic theory has been widely accepted governing the diamond growth in various CVD systems, there are different interpretations of key species for different CVD system. In HFCVD and MPCVD systems with methane/hydrogen mixture as precursors, the absorption and desorption of atomic hydrogen associated with the addition of hydrocarbon species, mostly likely CH_3, was suggested to kinetically control the construction of the diamond structure.[14,19] In combustion system, the addition of oxygen and the high volume of hydrocarbon precursor lead to a distinct gas phase. Methyl, CH_3, the main growth species in HFCVD and MPCVD was found inadequate for explaining the growth rate in combustion flames. Higher hydrocarbons were suggested to account for the diamond growth based on a good agreement to the deposition rate.[13,16] In this work, we found CH_3 concentration was below 0.25%. The concentrations of low hydrocarbons, which showed a similar variation with CH_3, increased as the deposition rate decreased. A role as growth species for low hydrocarbons was therefore not suggested. High hydrocarbons exhibited a good agreement with the deposition rate upon the control parameters, h and R, suggesting the involvement of higher hydrocarbons in diamond growth. The h-dependence and R-dependence of chemical intermediates and diamond deposition suggested a proper ratio between high hydrocarbons and carbon etchants was required for high-quality diamond growth. A kinetic competition process between growth and etching directed the diamond growth behaviour. Based on the MS results, diamond films were obtained within a well-defined window of the chemical intermediates as summarized in Table 1. With a low concentration of carbon etchants and a high concentration of high hydrocarbons, amorphous carbon is obtained. With a high concentration of carbon etchants and low concentration of high hydrocarbons, surface etching or no deposition occurs. The close correlation of the carbon etchants (H_3O^+, OH^-, and O^-) and high hydrocarbons ($C_2H_2^+$, $C_3H_3^+$, $C_3H_4^+$, $C_4H_2^+$, $C_4H_3^+$) with the deposition behaviour suggested their importance in diamond synthesis in combustion diamond synthesis.

Table 1. Relative concentration of active species in different combustion growth regimes

Species		Relative concentration (%)		
		Amorphous	Diamond	No growth
High hydrocarbons		>12.19	10.03-12.19	<10.03
Carbon etchants	H_3O^+	<7.33	7.33-12.77	>12.77
	OH^-	<2.74	2.74-5.98	>5.98
	O^-	<1.95	1.95-3.32	>3.32

Conclusions

In summary, the diamond growth and the relative concentration profiles of the chemical intermediates in the flames investigated using MS suggested a well-defined window of the chemical intermediates for effective diamond deposition. Beyond this window, either graphitic carbon deposition (overabundance of hydrocarbon-related intermediates) or no carbon deposition (overabundance of the etching species) occurred. A balance had to be established between the growth and the etching of diamond and graphitic carbon for producing high-quality diamond at a fast deposition rate. The resonant vibrational excitation at the wavelength of 10.532 μm was efficient in exciting the C_2H_4 molecules and enhancing the deposition rate. MS measurements of the flames under laser excitations at different lase wavelengths centred at 10.532 μm demonstrated that the resonant vibrational excitation effectively promoted the concentrations of the high hydrocarbons intermediates and suppressed the yield of carbon etchants, therefore resulted in the promoted diamond growth rate.

Acknowledgements

This research work was financially supported by National Science Foundation (CMMI 1129613 and 1068510) and Office of Naval Research (N00014-09-7581-0943).

Notes and references

[a] Department of Electrical Engineering, University of Nebraska-Lincoln, Lincoln, Nebraska, 68588-0511, USA.
[b] Institute de Chimie de la Matière Condensée de Bordeaux, Université de Bordeaux, 33608 Pessac cedex, France.

Electronic Supplementary Information (ESI) available: Experimental details of diamond film growth. Raman spectra of diamond films deposited as the functions of *h* and *R*, respectively. See DOI: 10.1039/b000000x/

1. J. Asmussen and D. K. Reinhard, *Diamond films handbook (Marcel Dekker: New York)*, 2002
2. J. J. Gracio, Q. H. Fan and J. C. Madaleno, *J. Phys. D: Appl. Phys*, 2010, **43**, 374017.
3. D. Choudhary and J. Bellare, *Ceram. Int.*, 2000, **26**, 73.
4. Y. Hirose and S. Amanuma, *J. Appl. Phys*, 1990, **68**, 6401.
5. A. G. Lowe, A. T. Hartlieb, J. Brand, B. Atakan and K. Kohse-Hoinghaus, *Combustion and Flame*, 1999, **118**, 37.
6. B. Atakan, and K. Kohse-Hoinghaus, *New Diamond and Frontier Carbon Technology,* 2001, **11**, 159.
7. K. Kohse-Hoinghaus, A. Lowe, B. Atakan, *Thin Solid Film,* 2000, **368**, 185.
8. R. J. H. KleinDouwel, J. J. L. Spaanjaars, J. J. ter Meulen, *J. Appl. Phys.* 1995, **78**, 2086.
9. L. C. Chen, P. D. Kichambare, K. H. Chen, J. J. Wu, J. R. Yang, and S. T. Lin, *J. Appl. Phys,* 2001, **89**, 753.
10. C. Benndorf, P. Joeris and R. Kroger, *Pure & Appl. Chem.* 1994, **66**, 1195.
11. S. W. Reeve, and W. A. Weiner, *J. Vac. Sci. Technol. A.* 1995, **13**, 359.
12. R. S. Yalamanchi, and K. S. Harshavardhan, *J. Appl. Phys.* 1990, **68**, 5941.
13. Y. Matsui, A. Yuuki, M. Sahara and Y. Hirose, *Japan J. Appl. Phys.* 1989, **28**, 1718.
14. W. L. Hsu, *Appl. Phys. Lett.* 1991, **59**, 1427.
15. R. S. Tsang, P. W. May, J. Cole, M.N.R. Ashfold, *Diamond Relat. Mater.* 1999, **8**, 1388.
16. C. A. Wolden, R. F. Davis, and Z. Sitar, *J. Mater. Res.* 1997, **12**, 2733.
17. C. A. Wolden, R. F. Davis, Z. Sitar and J. T. Prater, *Diamond Relat. Mater.* 1998, **7**, 133.
18. S. W. Reeve, and W. A. Weiner, *J. Appl. Phys.* 1993, **74**, 7521.
19. F. G. Celli, P. E. Pehrsson, H. T. Wang, J. E. Butler, *Appl. Phys. Lett.* 1988, **52**, 2043.
20. S. J. Harris, A. M. Weiner, and T. A. Perry, *Appl. Phys. Lett.* 1988, **53**, 1605.
21. S. F. Harris, *Appl. Phys. Lett.* 1990, **56**, 2298.
22. S. J. Harris, and A. M. Weiner, *Appl. Phys. Lett.* 1989, **55**, 2179.
23. D. G. Goodwin, and G. G. Gavillet, *J Appl. Phys.* 1990, **68**, 6393.
24. J. E. Butler and R. L. Woodin, *Journal TitlePhil. Trans. R. Soc. Lond. A.* 1993, **342**, 209.
25. J. S. Kim, and M. A. Cappelli, *J. Appl. Phys.* 1992, **72**, 5461.
26. M. Frenklach and K. E. J. Spear, *Mater. Res. 1988*, **3**, 133.
27. Y. Lifshitz, T. Kohler, T. Frauenheim, I. Guzmann, A. Hoffman, R. Q. Zhang, X. T. Zhou and S. T. Lee, *Science*, 2002, **297**, 1533.
28. B. V. Derjaguin and D. B. Fedoseev, *Sci. Am.* 1975, **233**, 102.
29. C. M. Marks, H. R. Burris, J. Grun and K. A. Snail, *J. Appl. Phys.* 1993, **73**, 755.
30. A. N. Hayhurst and D. B. Kittelson, *Combustion and Flame*, 1978, **31**, 37.
31. Z. Q. Xie, Y. S. Zhou, X. N. He, Y. Gao, J. Park, H. Ling, L. Jiang and Y. F. Lu, *Cryst. Growth Des.* 2010, **10**, 1762.
32. W. L. Smith and I. M. Mills, *J. Chem. Phys.* 1964, **40**, 2095.
33. H. J. Fissan, *Combustion and Flame*, 1971, **17**, 355.
34. R. Fridman and E. Burke, *J. Chem. Phys.* 1954, **22**, 824.
35. N. Uchida, T. Kurita, H. Ohkoshi, K. Uematsu and K. Saito, *J. Crsty. Growth*, 1991, **114**, 565.
36. A. V. Orden and R. J. Saykally, *Chem. Rev.* 1998, **98**, 2313.
37. W. J. Weltner and R. J. Van-Zee, *Chem. Rev*, 1989, **89**, 1713.
38. G. Bak, K. Fabisiak, L. Klimek, M. Kozanecki and E. Staryga, *Opt. Mater.* 2008, **30**, 770.
39. A. C. Ferrari and J. Robertson, *Phil. Trans. R. Soc. Lond. A*, 2004, **362**, 2477.
40. J. Schwan, S. Ulrich, V. Baori and H. Ehrhardt, *J. App. Phys.* 1996, **80**, 440.
41. A. N. Hayhust and N. R. Telford, *Nature-Phys. Sci*, 1972, 2**35**, 114.

42. R. A. Hepper, F. L. Walls, W. T. Armstrong and G. H. Dunn, *Phys. Rev. A*, 1976, **13**, 1000.
43. D. M. Gruen, P. C. Redfern, D. A. Horner, P. Zapol and L. A. Curtiss, *J. Phys. Chem.* 1999, **103**, 5459.
44. L. S. Fan, Y. S. Zhou, M. X. Wang, Y. Gao, L. Liu, J. F. Silvain and Y. F. Lu, *Laser Phys. Lett.* 2014, **11**, 076002.

Journal Name

RSCPublishing

ARTICLE

Table of Contents Image